Anharmonicity and lattice coupling of bond-centered hydrogen and interstitial oxygen defects in monoisotopic silicon crystals

R. N. Pereira* and B. Bech Nielsen
Institut for Fysik og Astronomi, Århus Universitet, DK-8000 Århus, Denmark

J. Coutinho and V. J. B. Torres
Department of Physics, University of Aveiro, Campus Santiago, 3810-193 Aveiro, Portugal

R. Jones
School of Physics, University of Exeter, Exeter EX4 4QL, United Kingdom

T. Ohya and K. M. Itoh
Department of Applied Physics and Physico-Informatics, Keio University and CREST-JST, Yokohama 223-8522, Japan

P. R. Briddon
School of Natural Sciences, University of Newcastle upon Tyne, Newcastle upon Tyne, NE1 7RU, United Kingdom
(Received 4 March 2005; published 28 September 2005)

We discuss the vibrational dynamics of bond-centered protons (H_{BC}^{+}) and deuterons (D_{BC}^{+}) in monoisotopic (^{28}Si, ^{29}Si, and ^{30}Si) silicon crystals, based on joint infrared absorption measurements and *ab initio* modeling studies. Protons and deuterons have been implanted at temperatures below 20 K, and *in situ*–type infrared absorption measurements have subsequently been performed at 8 K. A major absorption line is observed at 1998 cm^{-1} after proton implantation, which has previously been ascribed to a local mode of H_{BC}^{+}. We find that the H_{BC}^{+} mode at 1998 cm^{-1} displays an anomalous (positive) frequency shift when the Si isotope mass is increased, unlike the analogous D_{BC}^{+} mode at 1448 cm^{-1}, which shows a negative shift. This effect cannot be described with a purely harmonic model. We show that the mode frequencies are accurately accounted for with a simple model based on a linear Si-H-Si structure when anharmonicity, volumetric effects due to the host-isotope mass, and the coupling of the Si-H-Si unit to the lattice are taken into account. Interstitial oxygen (O_i) atoms in silicon, also located at the bond-center site, are as well investigated in a parallel way. The relative contributions of the different terms of the vibrational model to the mode frequency of H_{BC}^{+} and O_i are compared. The anomalous (positive) isotope shift of H_{BC}^{+} results from mixing via anharmonicity of A_{2u} and A_{1g} modes of the Si-H-Si unit, which shows that a reliable vibrational model has to take into consideration the local structure of the defect. The mode frequency of the O_i defect exhibits the normal (negative) isotope shift, because the relatively modest contribution of anharmonicity diminishes the importance of the mode mixing. The effect of the defect-lattice coupling on the stretch-mode frequencies of H_{BC}^{+} and O_i is also discussed.

DOI: 10.1103/PhysRevB.72.115212 PACS number(s): 61.72.Ji, 61.72.Bb, 74.62.Dh, 36.20.Ng

I. INTRODUCTION

The background for the interest in point defects in semiconductors is both fundamental and technological. Among the point defects, the class of hydrogen-related defects is of interest. Hydrogen is known to react with many other defects, including dopants, and to modify their electrical and optical properties by passivating, displacing, or even activating electrical levels.[1–3] The presence of such defects involving light impurity atoms frequently leads to the appearance of local vibrational modes (LVMs), with frequencies that mostly depend on the binding properties and effective mass of the impurity atoms. Therefore, the study of LVMs combined with isotope substitutions is particularly valuable as it provides an unambiguous fingerprint of the light elements involved in a defect.

LVMs of impurity defects are commonly discussed within the harmonic approximation and assuming that the defect local structure may be reduced to that of a diatomic system. In the diatomic model, one atom represents the impurity and the other represents the crystal host atoms to which the impurity is bonded. The frequency shifts that result when the isotope mass of the impurity and/or ligand atoms is changed (*isotope shifts*) may easily be calculated within this approximation, where the vibrational frequency is proportional to the inverse of the square root of the oscillator effective mass. Although often satisfactory, this approach is inadequate to describe light-element dynamics, where anharmonicity may account for up to 10% of the mode frequency. In such cases, anharmonicity strongly affects isotope shifts. A further complication is that a suitable description of defect vibrational dynamics has to consider how local modes are affected by the surrounding lattice. This defect-host coupling has commonly been accounted for by scaling the mass of the host species with an empirical parameter, known in the literature as the defect-lattice coupling parameter χ.[4] In combination with the χ parameter, the two-atom harmonic model has been very successful in describing LVMs of simple impurity-

defects. However, for strongly anharmonic systems the model parameters, i.e., the harmonic force constants and χ, become *contaminated* with anharmonicity (see Sec. III). Moreover, in some cases the defect vibration problem cannot be reduced to that of a diatomic molecule and, therefore, local structure of the defect has to be considered explicitly, as will be shown below. The recent availability of quasimonoisotopic Si crystals[5] opens prospects for the investigation of the host-mass dependence and the anharmonic properties of defect-related vibrations. Moreover, the effect of defect-lattice coupling on the impurity-related LVM frequencies may be better understood. In very recent investigations, the study of quasimonoisotopic Si crystals have revealed richer physics and subtleties that are unattainable in natural material. Examples are the reported anomalous isotope shifts that result from the volume dependence on the host isotope-species,[6] or the assignment of radiation-induced optical data to small self-interstitial aggregates in Si.[7]

In this paper we report on a detailed study of the LVMs of H_{BC}^{+} in monoisotopic silicon, for which we observe an anomalous positive shift of the stretching frequency when the Si isotope is increased. We present a combined experimental and *ab initio* modeling study of how anharmonic effects and the coupling of the H_{BC}^{+} to the lattice affect the stretch modes of this defect in silicon. The H_{BC}^{+} defect in silicon is an interesting case study because (i) hydrogen is the lightest element and large anharmonic effects are expected, (ii) the structure of H_{BC}^{+} is well established, and perhaps more importantly (iii) the large mass difference between the two stable isotopes implies a considerable reduction of the anharmonic contribution when hydrogen is replaced by deuterium (D). In order to get a better insight into the problem, we extended the investigations to include the interstitial oxygen (O_i) defect in silicon. Its structure is rather similar to that of H_{BC}^{+}, but the relative difference between the masses of the ^{16}O and ^{18}O isotopes is drastically smaller than for H and D.

Hydrogen in silicon occupies the bond-center position between two bonded Si atoms in the neutral and positive charge states, which results in defects with D_{3d} symmetry. The bond-centered hydrogen is the most fundamental hydrogen-related defect in silicon and it has been characterized in great detail both by experimental[8–14] and theoretical[15–19] methods. In the positively charged hydrogen defect, the two electrons occupy a three-center bond $sp^3(\mathrm{Si})+s(\mathrm{H})+sp^3(\mathrm{Si})$, which results from the symmetric combination of the two Si sp^3 hybrids and the hydrogen 1*s* orbital, whereas in the neutral-charge state the additional electron enters the antibonding state $sp^3(\mathrm{Si})$-$sp^3(\mathrm{Si})$. In natural silicon, H_{BC}^{+} gives rise to a major absorption line at 1998 cm^{-1}.[11,20] Analogously, a corresponding D_{BC}^{+}-related vibrational line appears at 1448 cm^{-1}. These bands arise from the asymmetric stretch modes of Si-H_{BC}^{+}-Si and Si-D_{BC}^{+}-Si, respectively, where the atoms vibrate along the $\langle 111\rangle$ trigonal axis. The H_{BC}^{+} defect is unstable at room temperature. However, it may be introduced at cryogenic temperatures by proton implantation and subsequently the defect may be detected by a record of the infrared absorbance spectrum without any intermediate heating of the sample.

The properties of oxygen in silicon have also been investigated extensively due to their importance in device engineering. It is generally accepted that interstitial oxygen in silicon occupies a bridging position between two Si atoms.[21–28] Although *ab initio* calculations indicate that the Si-O-Si unit has a slightly puckered form in the *frozen* ground-state structure,[24–28] they also predict a very small energy barrier to move the oxygen atom through the bond-center site. Actually, after considering zero-point energy motion, the O_i defect effectively assumes a linear Si-O-Si structure.[23,27] Interstitial oxygen is responsible for a prominent IR absorption band located at 1136 cm^{-1} at cryogenic temperatures. This band is attributed to the Si-O-Si asymmetric stretch mode,[22,23] i.e., it is analogous to the 1998 -cm^{-1} band of H_{BC}^{+} in silicon.

This paper is organized as follows. Section II describes the details about the experiments and consequent data. In Sec. III we briefly review the diatomic model that is commonly used to describe LVMs of impurity-defects and discuss its applicability to the case of H_{BC}^{+} in silicon. In Sec. IV we introduce the defect vibrational model that explains the isotope shifts observed for the H_{BC}^{+} mode frequencies. This includes the lattice-defect coupling and harmonic and anharmonic contributions. Section V contains the details and results of the *ab initio* calculations, and finally, we discuss and summarize the results in Sec. VI.

II. EXPERIMENTAL DETAILS AND RESULTS

In the present work we used isotopically enriched ^{28}Si (enriched to 99.93%), ^{29}Si (enriched to 97.10%), and ^{30}Si (enriched to 99.75%) crystals grown by the Czochralski method.[5] Samples with dimensions of approximately $8\times8\times0.7$ mm^3 were cut from the three crystals, and were mechanically polished on the two opposing 8×8 mm^2 faces to ensure maximum transmission of the infrared light.

The samples were mounted in a cryostat equipped with two CsI windows and one 0.2-mm-thick aluminium window. The cryostat was placed inside a vacuum chamber, which in turn was connected to the accelerator beam line. The samples were kept in good thermal contact with the cold finger of a closed-cycle helium cryocooler, which allowed us to keep the sample temperatures below 20 K during implantation. The samples were implanted through the aluminum window on one of the 8×8 mm^2 faces with protons (or deuterons) with different energies in the range 5–10 MeV. The implants were done sequentially from high to low energies, and the energy step and doses at each energy were adjusted to result in a nearly homogenous hydrogen (or deuterium) concentration of 10^{18}–10^{19} cm^{-3} in the range 150–550 μm below the surface. The ion beam was swept vertically and horizontally in order to obtain a uniform lateral distribution of the implanted species. At each energy, the beam current was measured before implantation with a beam cup, and the time of the implant was estimated taking into account the measured current and the desired dose. After the implantation, the cryostat was moved to the infrared spectrometer, while keeping the sample temperature below 20 K. This *in situ*–type procedure prevented hydrogen (or deuterium) from migrating and reacting with other defects.

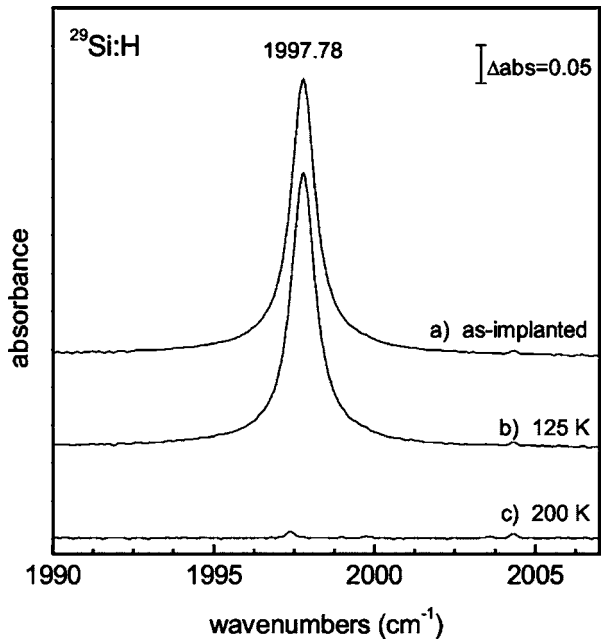

FIG. 1. Absorbance spectra recorded at 8 K on the ^{29}Si-enriched sample (a) after implantation with protons at $T<20$ K and after 30 min. annealing at (b) 125 K and (c) 200 K.

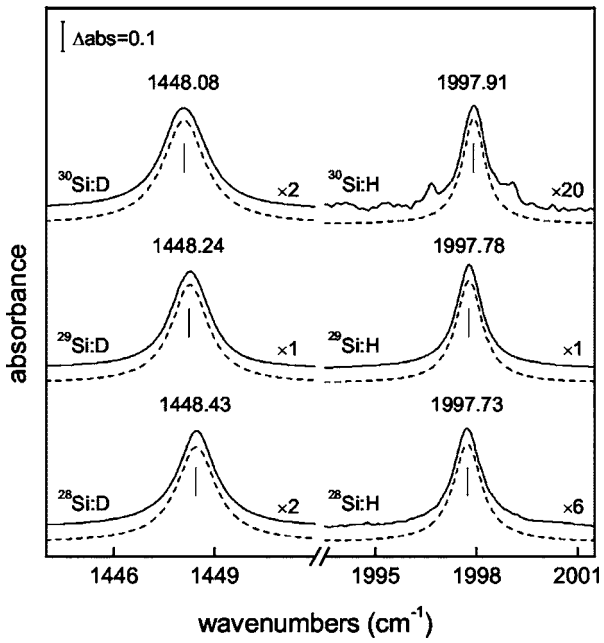

FIG. 2. Sections of absorbance spectra measured at ~8 K on proton- and deuteron-implanted ^{28}Si (^{28}Si:H and ^{28}Si:D), ^{29}Si (^{29}Si:H and ^{29}Si:D), and ^{30}Si (^{30}Si:H and ^{30}Si:D) crystals.

The infrared absorption measurements were carried out with a Nicolet System 800 Fourier-transform spectrometer, equipped with a glowbar light source, a Ge-KBr beam splitter, and a mercury-cadmium-telluride detector. In this configuration, the spectrometer covered the spectral range from 600 to 4000 cm^{-1}. All the spectra were obtained at ~8 K with an apodized resolution of 0.25 cm^{-1}. Intense water-related absorption lines were removed from the spectra by subtraction of a water reference spectrum measured with the same acquisition parameters.

After proton implantation a dominant absorbance line is observed at about 1998 cm^{-1} in all samples. This absorption line is shown in Fig. 1 for the ^{29}Si sample. The 1998-cm^{-1} line anneals out after heat treatments above 200 K. The value of the frequency as well as its annealing behavior confirm that this line represents the excitation of the asymmetric stretch mode of H^+_{BC}.[11,20]

In Fig. 2, sections of the absorbance spectra recorded on the ^{28}Si, ^{29}Si, and ^{30}Si samples after low-temperature proton and deuteron implantation are compared. In order to achieve an accurate determination of the frequencies of the modes for the different silicon isotopes, the experimental line shapes were fitted to Lorentzian profiles and the resulting best fits are represented by dashed lines in Fig. 2. We note that when the mass of the host species are changed the H^+_{BC} and D^+_{BC} bands shift in opposite directions. The frequency of the H^+_{BC} mode increases slightly when the silicon mass increases, whereas the D^+_{BC} mode frequency decreases. This puzzling observation will be discussed below.

III. THE DIATOMIC MODEL AND LATTICE-COUPLING PARAMETER

The LVM frequencies induced by impurity-defects in semiconductors are commonly described with the help of a model that considers a diatomic molecule *X*-*Y* with harmonic frequency $\omega^{\text{mol}}_{\text{harm}}$,[4]

$$\omega^{\text{mol}}_{\text{harm}} = \sqrt{\frac{F}{M_{\text{mol}}}} \tag{1}$$

with

$$\frac{1}{M_{\text{mol}}} = \frac{1}{m_X} + \frac{1}{\chi m_Y}, \tag{2}$$

where m_X and m_Y are the masses of the impurity *X* and host atoms *Y*, respectively, and the harmonic effective force constant of the oscillator is *F*. In the framework of this model the defect-host coupling is accounted for by scaling the mass of the ligand species by the empirical parameter χ. The parameters *F* and χ may be obtained from a fit of Eq. (1) to experimental LVM frequencies. The value of χ depends on (i) the number of atoms that neighbors the impurity, as well as on (ii) the defect-host coupling. Despite the impossibility of separating the effects (i) and (ii), this formalism has been applied successfully in describing isotope shifts on LVMs for simple defects like substitutional impurities in silicon,[29,30] and hydrogen-related defects in gallium arsenide.[4]

A problem with this approach originates from the fact that when both χ and *F* are obtained from a fit to isotope data, they become contaminated by anharmonic effects. For example, the hydroxyl free radical has an O-H stretch mode at 3568.0 cm^{-1} (for OH^-) and at 2632.1 cm^{-1} (for OD^-), leading to $F=42.68$ eV/Å^2 and $\chi=0.6446$, which is far off from the expected value $\chi=1.0$. On the other hand, the observation of *hot* vibrational bands allowed the estimation of the harmonic frequencies at 3735.21 cm^{-1} (for OH^-), and 2720.9 cm^{-1} (for OD^-). These correspond to rather different

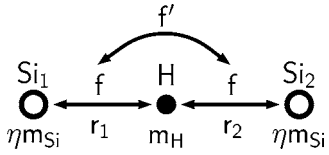

FIG. 3. A sketch of the Si-H-Si triatomic unit used as a defect model.

values of $F=48.16\ \mathrm{eV/\AA^2}$ and $\chi=0.9576$, which is now close to 1.

Another drawback of the theoretical approach of Eq. (1) is that for some complexes it is not possible to describe the vibrational properties accurately enough with a simple two-atom model, even when anharmonicity is taken into account. This is demonstrated by comparing the defect mode to that of an anharmonic diatomic molecule, for which the frequency may be written as[4]

$$\omega_{\mathrm{mol}} = \omega_{\mathrm{harm}}^{\mathrm{mol}} + \omega_{\mathrm{anharm}}^{\mathrm{mol}} = \sqrt{\frac{F}{M_{\mathrm{mol}}}} + \frac{A_{\mathrm{mol}}}{M_{\mathrm{mol}}}, \tag{3}$$

where F and M_{mol} stand for the effective force constant and effective mass of the diatomic oscillator, and A_{mol} is the anharmonic parameter, which is normally negative. It is easily seen from Eq. (3) that when the m_Y mass is increased the harmonic term contributes with a negative shift to ω_{mol}, whereas the anharmonic contribution to the isotope shift is positive. For small changes in the host mass m_Y, the magnitude of the ratio between the anharmonic ($\Delta\omega_{\mathrm{anharm}}^{\mathrm{mol}}$) and harmonic ($\Delta\omega_{\mathrm{harm}}^{\mathrm{mol}}$) isotope shifts is

$$\left|\frac{\Delta\omega_{\mathrm{anharm}}^{\mathrm{mol}}}{\Delta\omega_{\mathrm{harm}}^{\mathrm{mol}}}\right| \approx 2\left|\frac{\omega_{\mathrm{anharm}}^{\mathrm{mol}}}{\omega_{\mathrm{harm}}^{\mathrm{mol}}}\right|. \tag{4}$$

The magnitude of $\omega_{\mathrm{anharm}}^{\mathrm{mol}}$ is always much less than 50% of $\omega_{\mathrm{harm}}^{\mathrm{mol}}$. Therefore, from Eq. (4) the magnitude of the harmonic isotope shift (negative) is always much larger than $\Delta\omega_{\mathrm{anharm}}^{\mathrm{mol}}$ (positive) and, hence, the diatomic anharmonic potential cannot account for the positive isotope shifts observed for the H_{BC}^{+} data. This suggests that one should apply the diatomic model with caution. In the following section, we introduce a simple model to describe the anomalous vibrational properties of the H_{BC}^{+} defect in silicon, which takes into consideration the specific local structure of this defect.

IV. VIBRATIONAL MODEL FOR H_{BC}^{+} IN SILICON

A. Harmonic model

In order to understand the observed isotope data, we introduce a model that is based on the Si-H-Si unit shown in Fig. 3. The displacement coordinates r_1 and r_2 define the streching of the two Si-H bonds with respect to the equilibrium situation. We note that the observed mode for H_{BC}^{+} at 1998 $\mathrm{cm^{-1}}$ corresponds to the hydrogen atom oscillating along the Si-H-Si axis (asymmetric stretch). This frequency is substantially higher than the Raman frequency in Si, and even higher than that expected for the bond bend vibration, where hydrogen oscillates in the {111}-plane perpendicularly to the Si-H-Si axis. Therefore, we will not consider the coupling between stretch- and bend-mode vibrations of the hydrogen atom. In addition, we will initially neglect the coupling of the Si-H-Si unit to the lattice. With these initial assumptions, the vibrational problem is reduced to that of a pair of Si-H coupled oscillators. Within the harmonic approximation, a Hamiltonian may be written as[31]

$$\mathcal{H}_{\mathrm{harm}} = -\frac{\hbar^2}{2}\sum_{i,j} G_{ij}\frac{\partial^2}{\partial r_i \partial r_j} + \frac{1}{2}\sum_{i,j} F_{ij} r_i r_j, \tag{5}$$

where $i,j \in \{1,2\}$ and

$$\mathbf{G} = \begin{pmatrix} \mu & -\mu_{\mathrm{H}} \\ -\mu_{\mathrm{H}} & \mu \end{pmatrix}, \quad \mathbf{F} = \begin{pmatrix} f & f' \\ f' & f \end{pmatrix}, \tag{6}$$

with

$$\mu_{\mathrm{H}} = \frac{1}{m_{\mathrm{H}}} \text{ and } \mu = \frac{1}{m_{\mathrm{H}}} + \frac{1}{m_{\mathrm{Si}}}. \tag{7}$$

Here, m_{H} and m_{Si} denote the hydrogen (or deuterium) and silicon atomic masses, respectively. The coupling to the lattice may be introduced in an *ad hoc* manner at this point. First, we may consider the force constants f and f' to be effective force constants, which have values that depend on the surrounding lattice. Moreover, the effective mass of the silicon neighbors of the bond-centered hydrogen will differ from that of a free silicon atom due to the contribution of the surrounding lattice. Therefore, we substitute μ given in Eq. (7) by

$$\mu = \frac{1}{m_{\mathrm{H}}} + \frac{1}{\eta m_{\mathrm{Si}}}, \tag{8}$$

where η is a factor accounting for the defect-lattice coupling (see Sec. III). It should be noted that in the general case η differs from the parameter of the diatomic model χ, because the latter also depends on the local structure of the defect. The mode frequencies of the triatomic system may be determined by solving the secular equation[31]

$$|\mathbf{GF} - \omega^2 \mathbf{I}| = 0, \tag{9}$$

with $\mathbf{I}$ representing the identity matrix. Thus, for a D_{3d} symmetric Si-H-Si oscillator, we find the frequencies for the asymmetric $\omega_{\mathrm{harm}}^{A_{2u}}$ and symmetric $\omega_{\mathrm{harm}}^{A_{1g}}$ stretch modes to be

$$\omega_{\mathrm{harm}}^{A_{2u}} = \sqrt{\frac{f-f'}{m_{\mathrm{eff}}}} \tag{10}$$

and

$$\omega_{\mathrm{harm}}^{A_{1g}} = \sqrt{\frac{f+f'}{\eta m_{\mathrm{Si}}}}, \tag{11}$$

where the effective mass of the oscillator m_{eff} is given by

$$\frac{1}{m_{\mathrm{eff}}} = \frac{2}{m_{\mathrm{H}}} + \frac{1}{\eta m_{\mathrm{Si}}}. \tag{12}$$

The normal coordinates for the two modes may be expressed as

$$Q_{A_{2u}} = \sqrt{\frac{m_{\text{eff}}}{2}}(r_1 - r_2) \quad \text{(asymmetric)}, \tag{13}$$

$$Q_{A_{1g}} = \sqrt{\frac{\eta m_{\text{Si}}}{2}}(r_1 + r_2) \quad \text{(symmetric)}. \tag{14}$$

The symmetric A_{1g} mode involves only oscillations of the two silicon atoms. Thus, this mode has a low frequency and the assumptions made above for the asymmetric mode are inadequate for this mode. For convenience, any vibrational frequency ω stated below refers to the A_{2u} asymmetric mode, unless stated otherwise. Note that since the structure of the H_{BC}^+ defect is well established, i.e., the H atom has two Si neighbors, the effects (i) and (ii) discussed in the previous section are *a priori* separated in Eqs. (10) and (12) by assigning a coupling constant η to each Si-H bond.

B. Anharmonic contributions

Equation (10) predicts a decrease of the asymmetric stretching frequency as the Si mass increases. Although this trend is observed for the D_{BC}^+ related band, it contrasts with the peak frequency of H_{BC}^+, which increases slightly when the Si mass increases (see Fig. 2). This behavior cannot be accounted for with a vibrational model solely based on harmonic terms.

The cubic U_3 and quartic U_4 terms in the potential energy for a linear Si-H-Si oscillator with inversion symmetry may be written as

$$U_3 = f_3(r_1^3 + r_2^3) + f_3'(r_1^2 r_2 + r_1 r_2^2), \tag{15a}$$

$$U_4 = f_4(r_1^4 + r_2^4) + f_4'(r_1^3 r_2 + r_1 r_2^3) + f_4'' r_1^2 r_2^2, \tag{15b}$$

where f_3, f_3', f_4, f_4', and f_4'' are cubic and quartic force constants. We treat the anharmonic terms U_3 and U_4 as perturbations to the zero-order Hamiltonian given in Eq. (5). The anharmonic contribution to the energy is calculated as the sum of the second-order correction to the cubic terms and the first-order correction to the quartic terms. We find that the frequency correction, ω_{anharm}, to the asymmetric harmonic frequency, ω_{harm}, has the following dependence on the silicon and hydrogen isotope masses:

$$\omega_{\text{anharm}} = \omega_{\text{anharm}}^A + \omega_{\text{anharm}}^B + \omega_{\text{anharm}}^C = \frac{A}{m_{\text{eff}}} + \frac{B}{\sqrt{\eta m_{\text{Si}} m_{\text{eff}}}} + \frac{C}{\eta m_{\text{Si}}}, \tag{16}$$

with m_{eff} given in Eq. (12) and the parameters A, B, and C given by (see the Appendix)

$$A = -\frac{3\hbar}{2}\left[\frac{(3f_3 - f_3')^2}{3(f^2 - f'^2)} - \frac{2f_4 - 2f_4' + f_4''}{2(f - f')}\right], \tag{17a}$$

$$B \simeq -\frac{3\hbar}{4}\left[\frac{(f_3 + f_3')(3f_3 - f_3')}{(f + f')\sqrt{f^2 - f'^2}} + \frac{(3f_3 - f_3')^2}{6(f - f')\sqrt{f^2 - f'^2}} - \frac{6f_4 - f_4''}{3\sqrt{f^2 - f'^2}}\right], \tag{17b}$$

$$C \simeq \frac{\hbar}{16}\frac{(3f_3 - f_3')^2}{(f - f')^2}. \tag{17c}$$

The origin of the individual terms in Eq. (17) becomes clear after rewriting U_3 and U_4 in normal coordinates $Q_{A_{1g}}$ and $Q_{A_{2u}}$, i.e.,

$$U_3 = 2a^3(f_3 + f_3')Q_{A_{1g}}^3 + 2ab^2(3f_3 - f_3')Q_{A_{1g}}Q_{A_{2u}}^2, \tag{18a}$$

$$U_4 = a^4(2f_4 + 2f_4' + f_4'')Q_{A_{1g}}^4 + 2a^2b^2(6f_4 - f_4'')Q_{A_{1g}}^2 Q_{A_{2u}}^2 + b^4(2f_4 - 2f_4' + f_4'')Q_{A_{2u}}^4, \tag{18b}$$

where

$$a = \frac{1}{\sqrt{2\eta m_{\text{Si}}}} \text{ and } b = \frac{1}{\sqrt{2m_{\text{eff}}}}.$$

From a comparison of Eqs. (17) and (18) it is seen that ω_{anharm}^A contains a contribution from a cubic term, which mixes the A_{1g} and the A_{2u} modes, in addition to a contribution from a quartic term, which does not mix the two modes. The other terms in Eq. (16), ω_{anharm}^B and ω_{anharm}^C, arise solely from terms of the potential energy that mix the two modes.

The force constants that define the potential energy are normally assumed to be independent of the mass of the host atoms. However, this will not be an adequate approximation in our case, because a change of isotope (and mass) of the host atoms leads to a small change in the volume (and lattice parameter) of the crystal due to anharmonicity. This in turn leads to a change in the force constants that enter in our calculation of $\omega_{\text{harm}}^{A_{2u}}$. We will lock all force constants at the value they have for the ^{28}Si crystal and then account for the change in the lattice parameter by adding a volumetric correction term ω_{vol} to the calculated frequencies for the ^{29}Si and ^{30}Si crystals.

The dependence of the Si lattice constant on the isotope mass has been accurately measured by the x-ray standing-wave technique.[32] At low temperatures ($\sim$30 K), the relative change in the lattice parameter $\Delta a/a$ is found to be $-3.0 \times 10^{-5}\Delta m_{\text{Si}}$, where Δm_{Si} is the change in the silicon isotope mass in atomic mass units relative to ^{28}Si. An identical change in the lattice parameter can be achieved by hydrostatic pressure P. Fortunately, Budde *et al.*[13] investigated the changes in the frequency of the 1998-cm^{-1} mode induced by uniaxial stress. The ratio between the frequency change and the change in hydrostatic pressure $\Delta\omega/\Delta P$ is equal to the trace of the piezospectroscopic tensor A associated with the mode of interest. For a trigonal defect, the trace of A is $\text{Tr}(A) = 3A_1$.[33] From the value of A_1 determined in the uniaxial stress measurements[13] we get that $\Delta\omega/\Delta P = 27 \pm 3$ cm^{-1}/GPa. Since the relative change in volume is $\Delta V/V = 3\Delta a/a = -9 \times 10^{-5}$ and the bulk modulus of silicon at low temperature is $B = 97.9$ GPa, we get that the volumetric correction may be expressed as

TABLE I. The measured (ω_{exp}) and volume-corrected ($\omega_{exp}-\omega_{vol}$) frequencies for the asymmetric stretch mode of H_{BC}^+ and D_{BC}^+ in ^{28}Si, ^{29}Si, and ^{30}Si enriched crystals (experimental error of ± 0.02 cm^{-1}). Under "Fit to experiments" we give the total frequencies (ω), the volume-independent frequencies ($\omega-\omega_{vol}$), and the harmonic frequencies (ω_{harm}) resulting from the best fit of the anharmonic model AM_{mod} [see Eq. (20)] to the experimental frequencies ω_{exp}, together with the harmonic frequencies (ω_{harm}) that result from the adjustment of the harmonic model HM_{mod} [see Eq. (10)] to the experimental frequencies. Frequencies $\omega-\omega_{vol}$ and ω_{harm} obtained from the best fit to the *ab initio* potential $U(r_1,r_2)$ are also reported (see Sec. V D). All frequencies are given in cm^{-1}. Respective potential parameters are given below each model.

			Fit to experiments				*Ab initio* calculations	
	Experimental data			AM_{mod}			AM_{calc}	
Isotope configuration	ω_{exp}	$\omega_{exp}-\omega_{vol}$	HM_{mod} ω_{harm}	ω	$\omega-\omega_{vol}$	ω_{harm}	$\omega-\omega_{vol}$	ω_{harm}
^{28}Si-H-^{28}Si	1997.73	1997.73	1999.66	1997.72	1997.72	2144.24	2005.9	2125.1
^{29}Si-H-^{29}Si	1997.78	1997.54	1997.88	1997.80	1997.56	2143.86	2005.8	2124.7
^{30}Si-H-^{30}Si	1997.91	1997.43	1996.22	1997.90	1997.42	2143.50	2005.7	2124.2
^{28}Si-D-^{28}Si	1448.43	1448.43	1450.49	1448.43	1448.43	1524.60	1448.4	1512.9
^{29}Si-D-^{29}Si	1448.24	1448.07	1448.04	1448.24	1448.07	1524.06	1448.0	1512.2
^{30}Si-D-^{30}Si	1448.08	1447.74	1445.74	1448.08	1447.73	1523.56	1447.7	1511.6
$f-f'$ (eV Å^{-2})			7.02753		8.43194		8.2611	
$A/10^{-15}$ (eV Å^{-2} s)					−1.32709		−0.95616	
$B/10^{-15}$ (eV Å^{-2} s)					−0.977912		−1.8320	
$C/10^{-15}$ (eV Å^{-2} s)					0.00000[a]		0.45395	
η			0.331107		1.72326		1.3802	

[a]Parameter fixed at this value during the fitting procedure.

$$\omega_{vol} = 0.24 \times \Delta m_{Si}\ (\text{cm}^{-1}). \tag{19}$$

This correction is of the same magnitude as the observed shifts on the hydrogen-mode frequencies when the Si isotopes are changed and, thus, the correction cannot be neglected in this context. Hence, we need to consider

$$\omega = \omega_{harm} + \omega_{anharm} + \omega_{vol}. \tag{20}$$

There are no uniaxial stress data available for the 1448-cm^{-1} mode corresponding to D_{BC}^+. For a simple harmonic oscillator the change in the frequency $\delta\omega$ when the force constant F is changed is given by $\delta\omega=\omega\delta F/2F$. The force constants do not depend on the mass of the hydrogen isotope and, thus, $\delta\omega$ is proportinal to ω. Therefore, we have assumed that the ratio between the volumetric correction for the deuterium and the hydrogen cases is equal to ω_D/ω_H.

In Table I, we report the measured absorption frequencies ω_{exp} of H_{BC}^+ and D_{BC}^+ together with the *corrected* frequencies $\omega_{exp}-\omega_{vol}$, which do not depend on the crystal volume. Two models were fitted to the measured absorption frequencies ω_{exp}: (i) the harmonic model (HM_{mod}) based on Eq. (10) and (ii) the anharmonic model (AM_{mod}) based on Eq. (20). The frequencies corresponding to the best fit obtained with the two models are summarized in Table I. As expected, the HM_{mod} not only fails to reproduce the opposite Si isotope shifts for hydrogen and deuterium, but also overestimates their magnitudes by a factor of 10–20. Furthermore, the value of the coupling parameter is $\eta=0.33$ according to HM_{mod}. This suggests that the effective mass of the silicon neighbors is only one-third of that of a free silicon atom, which is unrealistically small, as will become clear below when we compare this with the results of the *ab initio* calculations in Sec. V. Clearly, a harmonic model is inadequate to account for the data.

According to Eqs. (10), (12), (16), and (20) the anharmonic model involves seven force constants together with the coupling parameter η. However, the frequency ω depends uniquely on only five parameters: the harmonic force constant $f-f'$; the anharmonic parameters A, B, and C; and the coupling constant η. These parameters may be obtained from a fit to the experimental frequencies. From a standard least-squares fitting procedure, we obtain the results shown in Table I (AM_{mod}). In this table we report ω, $\omega-\omega_{vol}$, and ω_{harm}, which stand for the total frequency, the volume-independent frequency, and the harmonic frequency contribution, respectively [see Eq. (20)]. We found that the contribution to ω_{anharm} arising from the last term in Eq. (16) is negligible for all realistic values of η, i.e., $1<\eta<2$. Therefore, this term was set equal to zero. Overall, the AM_{mod} reproduces the measured frequencies ω_{exp} of all isotope combinations within only 0.02 cm^{-1}. This may be compared with the ~ 2 cm^{-1} discrepancy obtained with the harmonic approximation (HM_{mod}). Further, the AM_{mod} accurately reproduces the magnitudes and signs of the Si isotope shifts observed for H_{BC}^+ and D_{BC}^+. One should note that the defect-lattice coupling parameter $\eta\approx 1.7$ is now considerably larger than 1.

It is instructive to compare the force constant $f-f'=8.43$ eV/Å^2 for each Si-H bond in H_{BC}^+, with those ob-

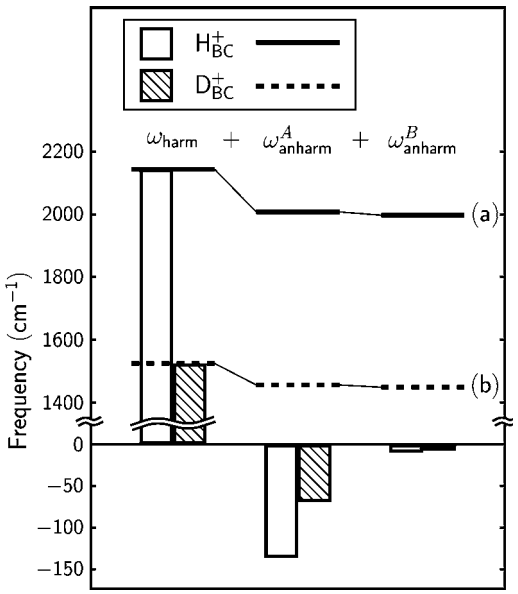

FIG. 4. Contribution of ω_{harm}, ω^A_{anharm}, and ω^B_{anharm} (bars) to the frequency of the asymmetric stretch mode of H^+_{BC} and D^+_{BC} defects in a ^{28}Si crystal obtained with the anharmonic model AM_{mod}. The results for H^+_{BC} and D^+_{BC} in ^{29}Si and ^{30}Si crystals are very similar. Added contributions to H^+_{BC} and D^+_{BC} frequencies are shown as solid (a) and dashed (b) lines, respectively.

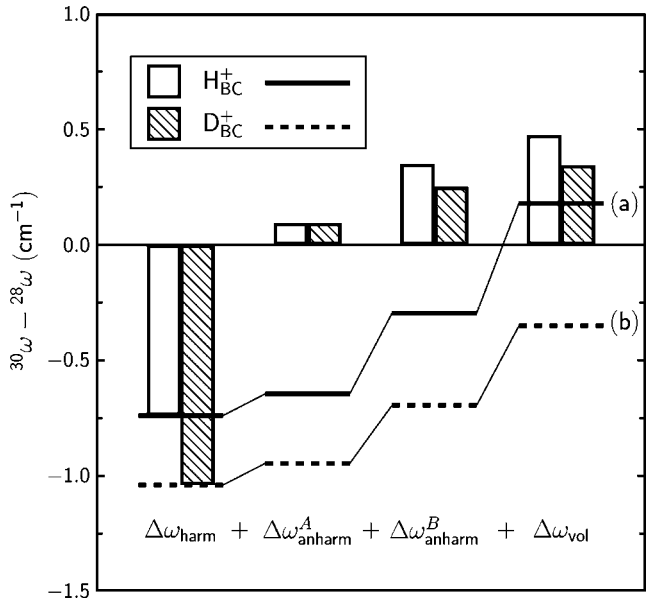

FIG. 5. Contributions (bars) of $\Delta\omega_{harm}$, $\Delta\omega^A_{anharm}$, $\Delta\omega^B_{anharm}$, and $\Delta\omega_{vol}$, to the $^{30}\omega$-$^{28}\omega$ isotope shift of the asymmetric stretch mode of H^+_{BC} and D^+_{BC}, found from the AM_{mod} parameters in Table I. Added contributions to the isotope shifts for H^+_{BC} and D^+_{BC} are shown as (a) solid and (b) dashed lines, respectively.

tained for the H^*_2 complex in Si. The latter forms two inequivalent and weakly coupled Si-H oscillators, with force constants 15.38 eV/Å^2 and 12.60 eV/Å^2.[34] These are almost twice as large as that found here for H^+_{BC}. We believe that this difference is caused by the fact that whereas each hydrogen atom in H^*_2 shares two electrons with their respective Si neighbors, H^+_{BC} has weaker Si-H bonds as only one electron is shared by each Si neighbor.

Figure 4 depicts in a cumulative way the contributions of ω_{harm}, ω^A_{anharm}, and ω^B_{anharm} to the total frequency ω for the ^{28}Si case. The anharmonic terms ω^A_{anharm} and ω^B_{anharm} contribute by about 5–7% to the total frequency, where ω^A_{anharm} is clearly dominant. Figure 5 shows the different anharmonic contributions to the isotope shift $\Delta\omega = {}^{30}\omega$-$^{28}\omega$ for the H^+_{BC} and D^+_{BC} frequencies, when the ^{28}Si enriched crystal is replaced by ^{30}Si material. As can be seen from the figure, the harmonic and anharmonic shifts have opposite signs. However, the total anharmonic shift ($\Delta\omega^A_{anharm}+\Delta\omega^B_{anharm}+\Delta\omega_{vol}$) surpasses the magnitude of the harmonic shift for H^+_{BC}, which results in an overall positive isotope shift. It is interesting to note that while ω^A_{anharm} dominates the anharmonic corrections to the absolute frequencies (see Fig. 4), it is $\Delta\omega^B_{anharm}$ and $\Delta\omega_{vol}$ that significantly contribute to the anharmonic frequency shift associated with a change of the silicon isotope.

C. Comparison with interstitial oxygen

The interstitial oxygen defect has also been investigated using the HM_{mod} and AM_{mod}. The trace of the piezospectroscopic tensor for this mode is only 2.31 cm^{-1}/GPa,[35] and the volumetric correction ω_{vol} is now negligible ($\sim 0.02 \times \Delta m_{Si}$ cm^{-1}). Therefore, this effect will be neglected here. The frequencies of the asymmetric stretch mode ω_{exp} were taken from Ref. 6 and are reproduced in Table II.

The frequencies obtained with the HM_{mod} agree well with the O_i absorption frequencies (see Table II). Discrepancies are below 0.4 cm^{-1} only. The Si isotope shift for $^{16}O_i$ is calculated to be about $-3.8 \times \Delta m_{Si}$ cm^{-1}, which is to be compared to $-3.7 \times \Delta m_{Si}$ cm^{-1} obtained from the measurements. The harmonic force constant $f-f'$ of the strong Si-O bond is about four times larger than that of the *single-electron* Si-H bond in H^+_{BC}.

The AM_{mod} slightly improves the agreement with the experimental frequencies (see Table II). As in H^+_{BC}, the term ω^C_{anharm} did not produce any significant effect on the overall frequency and was set to zero. We found that for O_i the anharmonic correction accounts for only 1.3% of the total frequency ω, with only a single dominant anharmonic term ω^A_{anharm}. Accordingly, the model predicts a harmonic frequency which lies about 15 cm^{-1} above the measured absorption frequency. One should note that Eq. (20) becomes similar to Eq. (3) of the two-atom anharmonic model, with $F=2(f-f')$, $\chi=2\eta$, and $A_{mol}=2A$, if the mode-mixing anharmonic terms ω^B_{anharm} and ω^C_{anharm} and the volumetric correction term ω_{vol} are neglected. Hence, the modest importance of anharmonicity in the asymmetric mode dynamics of O_i, makes the diatomic-molecule model already suitable to treat this defect. Finally, we note that the value of η is close to 1.2, suggesting a weaker defect-lattice coupling than for H^+_{BC}. This observation will be discussed in more detail below (see Sec. VI).

TABLE II. Experimental frequencies (ω_{exp}) for the asymmetric stretch mode of O_i in ^{28}Si, ^{29}Si, and ^{30}Si enriched crystals (taken from Ref. 6), along with the total frequency (ω) and harmonic frequency ω_{harm} resulting from the adjustment of the harmonic model (HM_{mod}) and the anharmonic model AM_{mod} to the experimental frequencies. Analogous values obtained from the $U(r_1,r_2)$ *ab initio* potential are also reported (see Sec. V D). All frequencies are given in cm^{-1}. Respective potential parameters are given below each model. NA stands for Not Available.

		Fit to experiments			*Ab initio* calculations	
			AM_{mod}		AM_{calc}	
Isotope configuration	Experimental data ω_{exp}	HM_{mod} ω_{harm}	ω	ω_{harm}	ω	ω_{harm}
^{28}Si-^{16}O-^{28}Si	1136.5	1136.6	1136.3	1152.5	1138.6	1152.0
^{29}Si-^{16}O-^{29}Si	1132.5	1132.7	1132.6	1148.7	1134.8	1148.1
^{30}Si-^{16}O-^{30}Si	1129.1	1129.0	1129.2	1145.1	1131.3	1144.6
^{28}Si-^{18}O-^{28}Si	1084.4	1084.7	1084.6	1099.4	1086.8	1098.9
^{29}Si-^{18}O-^{29}Si	1081.0	1080.6	1080.8	1095.4	1082.8	1094.9
^{30}Si-^{18}O-^{30}Si	NA	1076.8	1077.1	1091.6	1079.2	1091.2
$f-f'$ (eV Å^{-2})		30.437	31.602		31.520	
$A/10^{-15}$ (eV Å^{-2} s)			−2.0445		−1.6482	
$B/10^{-15}$ (eV Å^{-2} s)			0.0000		−0.25157	
$C/10^{-15}$ (eV Å^{-2} s)			0.0000[a]		0.37009	
η		1.1518	1.2106		1.2002	

[a]Parameter fixed at this value during the fitting procedure.

V. *AB INITIO* MODELING OF H_{BC}^{+} AND O_i DEFECTS IN SILICON

A. Calculational details

Structural and vibrational properties of H_{BC}^{+} and O_i defects in Si are calculated with a density functional code (AIMPRO),[36] along with the Padé parameterization for the local-density approximation[37] and the dual-space separable pseudopotentials by Hartwigsen, Goedecker, and Hutter.[38] Defects were embedded in a 216-atom supercell and in a bond-centered $Si_{148}H_{98}$ hydrogen-terminated cluster. Their ground-state structures were obtained by allowing all atomic positions to relax so to minimize the forces. In the cluster method, Si-H surface units were not allowed to move. In the supercell calculations, the Brillouin zone was sampled at the MP-2^3 special **k** points,[39] and plane waves with energies of up to 150 Ry were used to evaluate the Hartree and potential terms. Kohn-Sham states were expanded with help of a set of *spd*-like Cartesian-Gaussian orbitals centered on each atom. Accordingly (4, 4, 2), (4, 4, 0), and (6, 6, 3) local basis sets were chosen for Si, H, and O atoms, respectively, where each triplet (n_s,n_p,n_d) stands for the number of *s*-, *p*-, and *d*-like functions.

The coupling constant η, introduced in Sec. IV A, may be estimated from Eq. (10) if harmonic frequencies for several isotope configurations of Si-H-Si (Si-O-Si) oscillators are available. Such frequencies are obtained from the *ab initio* method, with the dynamical matrix elements being evaluated by displacing H and a selected number of Si neighbors along all three Cartesian axes by ±0.1 atomic units.[40] In order to attain a converged value of η, it is important to determine how many Si atoms should be included in the dynamical matrix. This was investigated in two ways: (i) By an *embedded cluster method* (ECM), where H (or O) and a number *N* of Si shells are embedded within a large H-terminated Si cluster. Here, H (or O) and the inner Si shells are allowed to vibrate and are coupled to the outer *frozen* atoms. The other way is (ii) a *free cluster method* (FCM), where the H_{BC} (or O_i) species, the *N* shells of Si neighbors, and the H-surface atoms (H_{surf}), are all allowed to vibrate. In order to minimize spurious effects from the H_{surf} atoms, the latter were decoupled from the cluster by setting all Si-H_{surf} and H_{BC}-H_{surf} (O_i-H_{surf}) force constants to zero. Values of $f-f'$ and η were then found from the calculated frequencies with help of Eq. (10). In these calculations we considered all combinations of ^{28}Si, ^{29}Si, ^{30}Si, H, and D (or ^{16}O and ^{18}O) isotopes.

We now describe the calculational details of the effective force constants for the harmonic model (HM_{calc}) and anharmonic model (AM_{calc}). These results are obtained by using 216-atom supercells plus the interstitial hydrogen at the bond-center site. The harmonic and anharmonic interatomic potential terms [Eqs. (5) and (15)], were calculated by displacing the H atom (or O atom), and its two immediate Si_1 and Si_2 neighbors by Δx_0, Δx_1, and Δx_2 along the [111] direction, respectively. The center of mass of the defect was kept at the bond-center site, i.e., enforcing $\Delta x_0 m_0 + \Delta x_1 m_1 + \Delta x_2 m_2 = 0$, where m_0, m_1, and m_2 are the atomic masses of H (or O), Si_1, and Si_2 atoms. The *ab initio* interatomic potential $U(r_1,r_2)$ was evaluated on a grid of 40×40 points with $-0.5 \leqslant r_1/\text{Å} \leqslant 0.5$ and $-0.5 \leqslant r_2/\text{Å} \leqslant 0.5$, where r_1 and r_2 are the same bond-displacement coordinates used in Eqs. (5) and (15). Finally, we obtain all harmonic and anharmonic

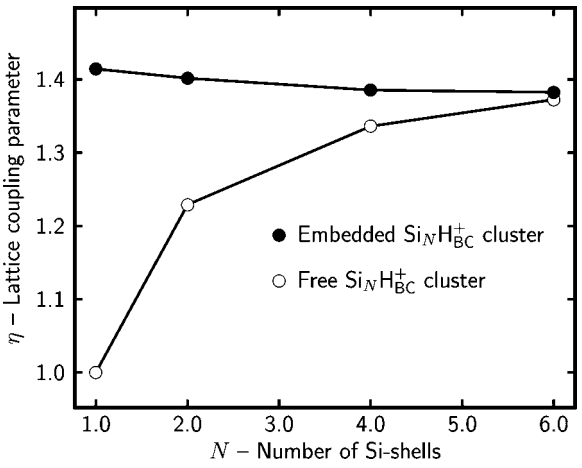

FIG. 6. Values of η determined from the harmonic *ab initio* frequencies, calculated according to the embedded cluster method ECM (closed circles) and the free cluster method FCM (open circles).

force constants by fitting Eqs. (5) and (15) to $U(r_1, r_2)$.

The fully relaxed ground-state structure of H^+_{BC} in Si is in line with previous reports.[18,41,42] Our supercell (cluster) results indicate that the defect has two equivalent 1.5893 Å (1.5872 Å) long Si-H bonds, increasing the separation between Si_1, and Si_2 atoms in Fig. 3 by about 36% with respect to the bulk Si-Si bond distance of 2.3344 Å (2.3287 Å). According to the supercell calculations, the interstitial oxygen defect occupies a slightly off-centered location, resulting in a Si-O-Si bent structure making an angle of ~155°. This structure is however only ~10 meV more stable than the perfect bond-centered form, also corroborating similar calculations reported earlier.[28] This energy difference is even smaller using the cluster method. Here we found degenerate off-centered and bond-centered forms, and unless otherwise stated, the latter will be assumed for the study of the vibrational properties of O_i. Here the supercell (cluster) calculations give Si-O bond lengths of 1.6139 Å (1.6099 Å), producing a larger 38% distortion on the perfect Si-Si nearest-neighbor distance.

B. Coupling constant η

The calculated values of the harmonic asymmetric (A_{2u}) stretch frequencies of H^+_{BC} and O_i defects in Si are close to those from other reports (see Refs. 28 and 43 and references therein). By considering six shells of Si atoms (or more) in the dynamical calculations, ECM gives A_{2u} mode frequencies at 2113 and 1156 cm^{-1} for ^{28}Si-H^+_{BC}-^{28}Si and ^{28}Si-$^{16}O_i$-^{28}Si complexes, respectively. These overestimate the low-temperature absorption data by about 115 and 20 cm^{-1}, but as expected, fall very close to the harmonic frequencies ω_{harm} at 2144 cm^{-1} and 1153 cm^{-1} estimated from the analysis of the absorption data within the anharmonic model AM_{mod} (see Tables I and II).

The calculated values of η for H^+_{BC}, and its dependence on the number of Si shells allowed to vibrate, are plotted in Fig. 6. Let us first look at the results from the FCM. When $N=1$, i.e., for a *free* triatomic Si-H-Si structure, η is expectedly 1.0. However, when the number of shells is increased, the value of η rises considerably and seems to converge to ~1.38. On the other hand, according to the ECM calculation we see that η is already about 1.4 for $N=1$. The difference from the FCM calculations is basically that now the Si-H-Si unit is coupled to a frozen host. The fact that η is much closer to its asymptotic value indicates that η is critically dependent on the coupling between H and second (and possibly further)–neighboring Si atoms. In both methods $f-f'$ and η converge to about 8.12 eV/Å^2 and 1.38, respectively, at $N=6$. Our best estimate of η is 1.3802, which corresponds to ECM at $N=6$, and will be used in the next subsections. Similar calculations were performed for O_i in Si, where we obtain asymptotic values $f-f'=31.74$ eV/Å and $\eta=1.20$. The value of $\eta=1.2002$ from the ECM calculation at $N=6$ will be used in the next subsections. The calculated values of η are in fair agreement with the AM_{mod} values shown in Tables I and II.

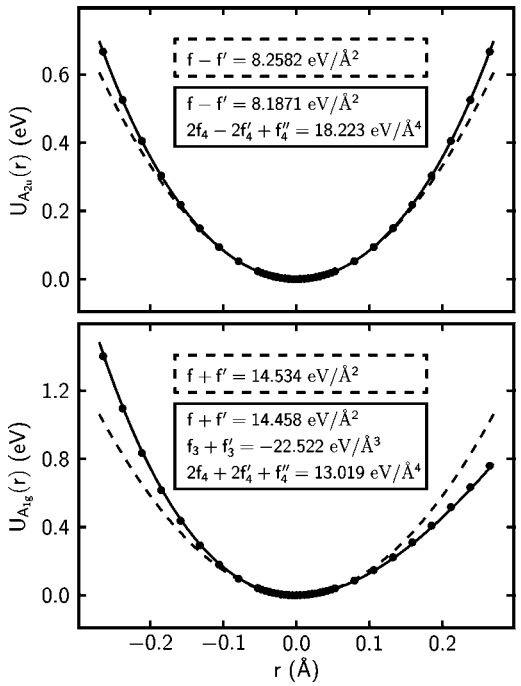

FIG. 7. Nonmixing anharmonic potentials (see Sec. V C) for H^+_{BC} in Si (solid lines), fitted to the *ab initio* total energy calculations of $U_{A_{2u}}(r)$ and $U_{A_{1g}}(r)$ (dots). Dashed curves result from a fit of the harmonic potential in Eq. (5) to the *ab initio* results within the harmonic region $|r|<0.05$ Å. Parameters from the anharmonic and harmonic fits are shown in solid and dashed boxes, respectively.

C. Independent-mode potential models

Now we report the harmonic and anharmonic properties of the Si-H-Si and Si-O-Si vibrating units. For the moment, no mode-mixing effects will be considered, with the A_{2u} and A_{1g} modes assumed as being independent. Accordingly, we displaced H (or O) and its two Si neighbors in accordance with their normal mode coordinates, i.e., with $r=r_1=-r_2$ for the A_{2u} mode and $r=r_1=r_2$ for the A_{1g} mode. Interatomic

TABLE III. Calculated force constants for H_{BC}^{+} and O_i, obtained from the *ab initio* nonmixing $U_{A_{2u}}(r)$ and $U_{A_{1g}}(r)$ potentials and mixing-mode $U(r_1,r_2)$ potential model. Harmonic, cubic, and quartic force constants are given in eV/Å^2, eV/Å^3, and eV/Å^4. Their relative uncertainties are about 0.2%, 1%, and 5%, respectively.

Potential	Force constant	H_{BC}^{+}	O_i
$U_{A_{2u}}(r=r_1=-r_2)$	$f-f'$	8.1871	31.501
	$2f_4-2f_4'+f_4''$	18.223	52.011
$U_{A_{1g}}(r=r_1=r_2)$	$f+f'$	14.458	37.634
	f_3+f_3'	−22.522	−36.273
	$2f_4+2f_4'+f_4''$	13.019	56.980
$U(r_1,r_2)$	$f-f'$	8.2611	31.520
	$2f_4-2f_4'+f_4''$	18.594	51.583
	$f+f'$	14.512	37.997
	f_3+f_3'	−22.803	−36.328
	$2f_4+2f_4'+f_4''$	12.769	57.074
	$3f_3-f_3'$	−27.442	−94.542
	$6f_4-f_4''$	50.043	360.04

potentials $[U_{A_{2u}}(r)$ and $U_{A_{1g}}(r)]$ were evaluated, with r chosen to lie within $|r|<0.3$ Å, and the results are shown in Fig. 7.

1. Harmonic model

Dashed lines in Fig. 7 represent the HM_{calc} interatomic potentials, and result from a fit of Eq. (5) to the $U_{A_{2u}}$ and $U_{A_{1g}}$ potentials within the harmonic region $|r|<0.05$ Å. From this we obtain the harmonic force constants $f-f'=8.2582$ eV/Å^2 and $f+f'=14.534$ eV/Å^2. With this value of $f-f'$ and the value $\eta=1.3802$ estimated above, the mode frequency for the HM_{calc} may be calculated using Eq. (10). Such calculation yields a frequency $\omega_{harm}=2124.8$ cm^{-1} for ^{28}Si-H_{BC}^{+}-^{28}Si, which is very close to the ECM calculation described above (2113 cm^{-1}).

Analogous calculations were performed for O_i. Here the force constants are $f-f'=31.342$ and $f+f'=37.870$, about 3–4 times larger than those of H_{BC}^{+}. Using the value $\eta=1.2002$ estimated above the HM_{calc} predicts $\omega_{harm}=1148.7$ cm^{-1} for ^{28}Si-$^{16}O_i$-^{28}Si, which again reproduces well the ECM calculation (1156 cm^{-1}).

2. Anharmonic model

Now we turn to anharmonic effects, but still ignoring terms in the potential energy that mix the A_{2u} and A_{1g} modes. Unlike for the A_{1g} mode, inversion symmetry implies that any cubic term vanishes in the A_{2u} mode. From Eq. (18), only the quartic term proportional to $2f_4-2f_4'+f_4''$ affects the asymmetric frequency, since we neglect mixing terms, and accordingly,

$$\omega=\sqrt{\frac{f-f'}{m_{\mathrm{eff}}}}+\frac{3\hbar}{2m_{\mathrm{eff}}}\left[\frac{2f_4-2f_4'+f_4''}{2(f-f')}\right]. \tag{21}$$

This indicates that the quartic term $2f_4-2f_4'+f_4''$ would have to be negative in order to account for the harmonic frequency lying above the experimental line frequency. Solid lines in Fig. 7 represent the fits of the anharmonic potential in Eqs. (5) and (15) to the total energy results $U_{A_{2u}}(r)$ and $U_{A_{1g}}(r)$ with $r=r_1=-r_2$ and $r=r_1=r_2$, respectively. The resulting harmonic and anharmonic parameters are reported in the upper half of Table III. The quartic term $2f_4-2f_4'+f_4''$ is positive for both H_{BC}^{+} and O_i, and we conclude that this correction alone cannot account for the measured mode frequency lying below the harmonic estimate. In fact, using Eq. (21) and the force constants for the $U_{A_{2u}}$ potential in Table III, we obtain frequencies ω for H_{BC}^{+} and O_i defects that overestimate the measurements by 230 cm^{-1} and 22 cm^{-1}, respectively.

As depicted in Fig. 4, the dominant anharmonic contribution to the absolute frequency is $\omega_{\mathrm{harm}}^{A}$. Its negative value is in apparent contradiction with the calculations described above. However, from Eqs. (17a) and (18), we conclude that the *key* correction must arise from the $A_{2u}+A_{1g}$ mixing term $3f_3-f_3'$, which up to this point has remained unexplored.

D. Mode-mixing effects

Parameters A, B, and C in Eq. (17) account for the mixing between A_{2u} and A_{1g} modes by means of cubic $(3f_3-f_3')$ and quartic $(6f_4-f_4'')$ force constants [see Eq. (18)]. As described at the beginning of Sec. V, these anharmonic force constants were calculated from the *ab initio* potential $U(r_1,r_2)$ on a 40×40 two-dimensional grid (r_1,r_2), with r_1 and r_2 representing the bond-displacement coordinates shown in Fig. 3. Results from these calculations are summarized at the bottom of Table III. Here we note that the harmonic $(f-f'$ and $f+f')$ and nonmixing anharmonic $(f_3+f_3'$, $2f_4-2f_4'+f_4''$, and $2f_4+2f_4'+f_4'')$ force constants are close to those obtained from the $U_{A_{2u}}$ and $U_{A_{1g}}$ nonmixing potentials. However, for both H_{BC}^{+} and O_i defects the force constants of the mixing terms $3f_3-f_3'$ and $6f_4-f_4''$ are not negligible.

The parameters A, B, and C obtained with Eq. (17) from the $U(r_1,r_2)$ potential parameters, given in Table III, are shown at the bottom of Table I under AM_{calc}. Noting that the relative error on the individual force constants is up to 5%, the agreement of the calculated parameters with the values obtained from AM_{mod} is satisfactory (see Table I). Using Eqs. (10) and (17), we can calculate the volume-independent *ab initio* frequencies $\omega-\omega_{vol}$ within the anharmonic model for the isotope combinations of interest. These are reported in Table I under AM_{calc}. As expected, the harmonic frequencies ω_{harm} from the AM_{calc} calculations are higher than the volume-corrected frequencies $\omega_{exp}-\omega_{vol}$ for Si-H-Si and Si-D-Si by about 115 and 55 cm^{-1}, respectively. However, after adding the anharmonic contributions, the calculated frequencies $\omega-\omega_{vol}$ reproduce the $\omega_{exp}-\omega_{vol}$ data to within less than ~8 cm^{-1}. The isotope shift $^{30}\omega-^{28}\omega$ of about -0.2 cm^{-1} for H_{BC}^{+}, which is calculated with the frequencies $\omega-\omega_{vol}$ of the AM_{calc}, is in excellent agreement with that observed for the $\omega_{exp}-\omega_{vol}$ data (-0.3 cm^{-1}). In addition, the small upward Si isotope shift observed for H_{BC}^{+} is readily accounted for by the theoretical calculations, if we include the ^{28}Si to ^{30}Si volume correction $\Delta\omega_{vol}\approx0.5$ cm^{-1}.

Good agreement is also obtained for O_i. For example, the AM_{calc} anharmonic frequencies ω shown in Table II repro-

duce the experimental frequencies within ~ 2 cm^{-1}. Also in O_i, the harmonic frequencies for Si-^{16}O-Si and Si-^{18}O-Si lie above the anharmonic-corrected values by ~ 20 cm^{-1} and ~ 15 cm^{-1}, respectively. Moreover, unlike in the H_{BC}^+ case, both harmonic (ω_{harm}) and fundamental transition (ω) frequencies account well (within less than 0.1 cm^{-1}) for the measured -7.4 cm^{-1} isotope shift in the $^{16}O_i$ mode frequency when ^{28}Si is replaced by ^{30}Si. This indicates that in comparison to H_{BC}^+, $A_{2u}+A_{1g}$ mode-mixing and volumetric effects are less important in O_i.

VI. DISCUSSION AND CONCLUSIONS

The vibrational properties of bond-centered hydrogen and deuterium defects in isotope enriched ^{28}Si, ^{29}Si, and ^{30}Si crystals have been studied experimentally and by *ab initio* theory. Mode frequencies were recorded for all isotope combinations and we found that the mode frequency for H_{BC}^+ shows an unusual increase when the mass of the host isotope is increased. The D_{BC}^+ mode, however, displays a normal isotope shift. Several models were tested, and it is shown that this effect can only be accounted for by anharmonic effects on a model based on the triatomic structure Si-H-Si. The relatively simple model reproduces the measured mode frequencies to within 0.03 cm^{-1}. We find that the anomalous (positive) isotope shift of the H_{BC}^+ mode frequencies result from mixing via anharmonicity of the A_{2u} and A_{1g} modes of the Si-H-Si structure. The H_{BC}^+ mode frequencies cannot be well reproduced within the diatomic molecule model and the two-bond local structure of the defect has to be taken into account. The investigations are extended to include the interstitial oxygen center in silicon, which has a very similar structure to H_{BC}^+. In the case of O_i the harmonic model gives already a good description of the experimental mode frequencies, and the inclusion of anharmonic effects in the model yields only a small improvement of the agrement of the calculated frequencies to the experimental data. The relatively modest importance of the anharmonicity in the vibrational dynamics of O_i yields a normal (negative) isotope shift for the O_i mode frequency when the host silicon isotope mass is increased.

Density functional calculations on H_{BC} and O_i defects are presented as well. Their vibrational properties were obtained according to three different methods. In the first method we use the harmonic approximation, and consider in the dynamical equations up to six shells of Si atoms neighboring the bond-centered hydrogen atom. In the second method we studied the anharmonic interatomic potential for the Si-H -Si (Si-O-Si) units. This was accomplished by varying the Si_1-H and Si_2-H (Si_1-O and Si_2-O) bond lengths along the symmetric A_{1g} and asymmetric A_{2u} normal modes. Finally, in the third method the bond lengths Si_1-H and Si_2-H (Si_1-O and Si_2-O) were varied independently in order to map the two-dimensional energy surface $U(r_1,r_2)$, where r_1 and r_2 are the stretch coordinates of the two Si-H (Si-O) bonds. All three methods predict similar harmonic frequencies ω_{harm} of ~ 2115 cm^{-1} for H_{BC}^+ and ~ 1150 cm^{-1} for O_i, exceeding the measured frequencies by about 115 cm^{-1} and 15 cm^{-1}, respectively. However, in line with the model analysis of the experimental data, the calculations show that those differences are reduced down to $2-8$ cm^{-1} if we include anharmonic effects (see Tables I and II). We show that the experimental Si isotope shifts of both H_{BC}^+ and O_i defects can be very well predicted with our AM_{calc} *ab initio* investigations.

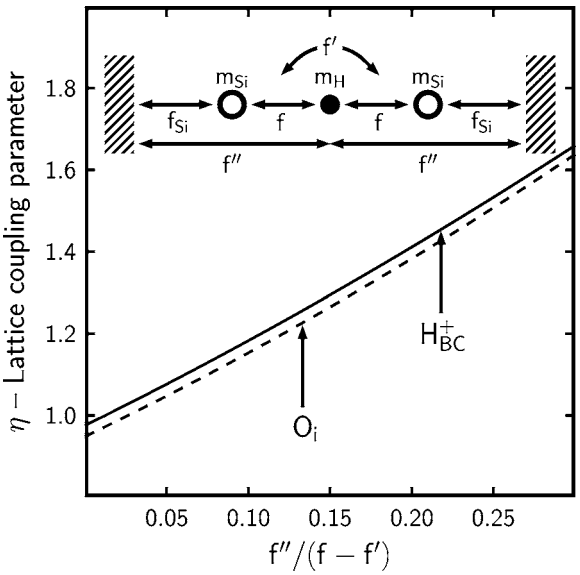

FIG. 8. Calculated dependence of the coupling constant η, introduced in the model of Fig. 3, on the interaction ratio $f''/(f-f')$ for H_{BC}^+ (solid line) and O_i (dashed line). Values of η were determined by setting the asymmetric stretch frequencies from the model depicted in the inset to those from Eq. (10). Upward arrows point to $f''/(f-f')=0.21$ and 0.13 obtained from the *ab initio* calculations for H_{BC}^+ and O_i, respectively.

The results presented in the previous sections raise several issues. For example, both our model analysis of the experimental data and *ab initio* theory indicate that the Si-O-Si oscillator is less coupled to the host crystal than the Si-H -Si defect, since the value of η determined for H_{BC}^+ is higher than that for O_i. Such a result seems contradictory with H_{BC}^+ having a smaller Si-isotope frequency shift than O_i, because this indicates a higher degree of localization for the H_{BC}^+ mode than for the O_i-related mode. Figure 6 clearly shows that a good estimate of η is already obtained if the interaction between the Si_1-H-Si_2 unit and the remaining (frozen) host atoms is included. Such an effect arises from two main contributions: (i) the lattice coupling with Si_1 and Si_2, and (ii) the H-lattice coupling. These couplings may be approximated with help from the model sketched in Fig. 8. Here, the effect of η on the mass of Si_1 and Si_2 atoms (see Fig. 3) is replaced by Si-lattice and H-lattice central potentials, represented by f_{Si} and f'' force constants, respectively. These represent springs fastened to fixed points (frozen lattice). The relation $\omega_{harm}^{A_{2u}}(f,f',f'',f_{Si})$ for the model shown in Fig. 8 was calculated, where the force constants f and f' are taken from the potential $U(r_1,r_2)$ (Table III). A fair estimate of the force constant f_{Si} is obtained from the Raman frequency in Si ($\omega_R=524.6$ cm^{-1}), by $f_{Si}=m_{Si}\omega_R^2/4=7.0716$ eV/Å^2. For every f'', we found the corresponding value of η by setting $\omega_{harm}^{A_{2u}}(f,f',f'',f_{Si})$ equal to $\omega_{harm}^{A_{2u}}$ in Eq. (10).

Figure 8 shows the resulting values of η as a function of the ratio between the H-lattice (O-lattice) force constant f''

and the Si-H (Si-O) force constant $f-f'$. The figure shows that independently of the defect, η is largely determined by the interaction ratio $f''/(f-f')$. We also found that the effect of f_{Si} on η is negligible. A 10% increase on f_{Si} results only in a 0.5% decrease of η. The magnitude of central force constant f'' may be estimated for each defect from the dynamical matrix of the ECM *ab initio* calculations. These are about 1.98 eV/Å^2 and 4.20 eV/Å^2 for H_{BC}^+ and O_i, respectively, resulting in $f''/(f-f')$ values indicated by the arrows in Fig. 8. These correspond to the calculated values of $\eta \approx 1.4$ for H_{BC}^+ and $\eta=1.2$ for O_i. In spite of the minute Si-isotope shifts on the 1998-cm^{-1} band (H_{BC}^+) when compared to those on the 1136-cm^{-1} band (O_i), it may be concluded that the larger defect-lattice coupling in H_{BC}^+ results from a larger interaction ratio $f''/(f-f')$.

Another issue is the role of the anharmonic terms that mix the A_{2u} and A_{1g} modes. Both the analysis of the experimental frequencies and *ab initio* theory indicate that the A_{2u} harmonic frequency of H_{BC}^+ lies well above the measured 1998-cm^{-1} mode frequency by 120–150 cm^{-1}. This is only possible if the $3f_3-f_3'$ mode-mixing force constant is considered in the dominant anharmonic correction $\omega_{\mathrm{anharm}}^A$ (see Fig. 4), as can be seen from Eq. (17a). Additionally, the volumetric frequency correction ω_{vol} associated with the crystal isotope, cannot alone account for the positive Si-isotope shift of the 1998-cm^{-1} band. Figure 5 clearly shows that the mode-mixing correction $\Delta\omega_{\mathrm{anharm}}^B$ is crucial to explain the overall shift. A similar negative contribution of the anharmonicity to the total frequency, although smaller in magnitude, is obtained from the model analysis of the experimental frequencies and predicted from *ab initio* calculations for O_i. However, as a result of the larger effective mass of the oscillator, mode-mixing effects are less important and the harmonic frequency lies only $\sim$15 cm^{-1} above the measured frequency. This, together with the negligible volumetric shift, results in a nearly harmonic Si-isotope shift of $-3.8\times\Delta m_{\mathrm{Si}}$ cm^{-1} for O_i.

ACKNOWLEDGMENTS

This work has been supported by the Danish National Research Foundation through the Aarhus Center for Advanced Physics (ACAP). R.N.P. thanks the ECCN network for support. J.C and V.J.B.T would like to acknowledge financial support from INTAS (Grant No. 03-50-4529) and the FCT in Portugal (Grants Nos. POCTI/CTM/40979/2001 and SFRH/BPD/5735/2001).

APPENDIX

The exact expressions for the parameters B and C which are calculated by treating the anharmonic terms of the potential U_3 and U_4 as perturbations to the Hamiltonian (5) are

$$B=-\frac{3\hbar}{4}\left[\frac{(f_3+f_3')(3f_3-f_3')}{(f+f')\sqrt{f^2-f'^2}}+\frac{2}{3}\sqrt{\frac{f-f'}{f+f'}}\frac{(3f_3-f_3')^2}{\Lambda}-\frac{6f_4-f_4''}{3\sqrt{f^2-f'^2}}\right], \tag{A1a}$$

$$C=\frac{\hbar}{4}\left[\frac{(3f_3-f_3')^2}{\Lambda}\right], \tag{A1b}$$

with

$$\Lambda=4(f-f')^2-\frac{m_{\mathrm{eff}}}{\eta m_{\mathrm{Si}}}(f^2-f'^2). \tag{A2}$$

By substitution of Eqs. (11) and (10), the ratio between the two terms of the right-hand side of Eq. (A2) may be written

$$\frac{m_{\mathrm{eff}}(f+f')}{4\eta m_{\mathrm{Si}}(f-f')}=\left(\frac{\omega_{\mathrm{harm}}^{A_{1g}}}{2\omega_{\mathrm{harm}}^{A_{2u}}}\right)^2. \tag{A3}$$

The frequency of the A_{1g} has not been detected, but the estimation from the *ab initio* calculations places this mode at 401 cm^{-1}, well below the Raman frequency in silicon (523 cm^{-1}). Taking the harmonic frequency of the A_{2u} mode $\omega_{\mathrm{harm}}^{A_{2u}}=2144$ cm^{-1} (see Table I), we find that

$$\left(\frac{\omega_{\mathrm{harm}}^{A_{1g}}}{2\omega_{\mathrm{harm}}^{A_{2u}}}\right)^2 \leqslant 0.01. \tag{A4}$$

Hence the second term in Eq. (A2) is at maximum 1% of the first term. It may safely be neglected, leading to the results given in Eqs. (17b) and (17c).

*Electronic address: pereira@phys.au.dk

[1] S. J. Pearton, J. W. Corbett, and M. Stavola, *Hydrogen in Crystalline Semiconductors* (Springer-Verlag, Berlin, 1992).

[2] *Hydrogen in Semiconductors*, edited by J. I. Pancove and N. M. Johnson, Semiconductors and Semimetals Vol. 34 (Academic Press, Boston, 1991).

[3] *Hydrogen in Semiconductors II*, edited by N. H. Nickel, Semiconductors and Semimetals Vol. 61 (Academic Press, New York, 1999).

[4] R. C. Newman, Physica B **170**, 409 (1991).

[5] K. M. Itoh *et al.*, Jpn. J. Appl. Phys., Part 1 **42**, 6248 (2003).

[6] J. Kato, K. M. Itoh, H. Yamada-Kaneta, and H.-J. Pohl, Phys. Rev. B **68**, 035205 (2003).

[7] S. Hayama, G. Davies, and K. M. Itoh, J. Appl. Phys. **96**, 1754 (2004).

[8] H. J. Stein, Phys. Rev. Lett. **43**, 1030 (1979).

[9] B. Holm, K. Bonde Nielsen, and B. Bech Nielsen, Phys. Rev. Lett. **66**, 2360 (1991).

[10] Y. V. Gorelkinskii and N. N. Nevinnyi, Mater. Sci. Eng., B **36**, 133 (1996), and references therein.

[11] M. Budde, Ph.D. thesis, Århus University, Denmark, 1998.

[12] K. Bonde-Nielsen, B. B. Nielsen, J. Hansen, E. Andersen, and J. U. Andersen, Phys. Rev. B **60**, 1716 (1999).

[13] M. Budde, G. Lüpke, C. P. Cheney, N. H. Tolk, and L. C. Feldman, Phys. Rev. Lett. **85**, 1452 (2000).

[14] M. Budde, C. P. Cheney, G. Lüpke, N. H. Tolk, and L. C. Feld-

man, Phys. Rev. B **63**, 195203 (2001).
[15] S. Estreicher, Phys. Rev. B **36**, 9122 (1987).
[16] C. G. Van de Walle, P. J. H. Denteneer, Y. Bar-Yam, and S. T. Pantelides, Phys. Rev. B **39**, 10791 (1989).
[17] R. Jones, Physica B **170**, 181 (1991).
[18] S. K. Estreicher, Mater. Sci. Eng., R. **R14**, 319 (1995).
[19] C. G. Van de Walle, in *Hydrogen in Semiconductors II*, Ref. 3, (Academic Press, New York, 1999), pp. 241–281.
[20] B. Bech Nielsen, K. Tanderup, M. Budde, K. Bonde Nielsen, J. L. Lindström, R. Jones, S. Öberg, B. Hourahine, and P. Briddon, Mater. Sci. Forum **258–263**, 391 (1997).
[21] J. Corbertt, R. McDonald, and G. D. Watkins, J. Phys. Chem. Solids **25**, 873 (1964).
[22] D. R. Bosomworth, W. Hayes, A. R. L. Spray, and G. D. Watkins, Proc. R. Soc. London, Ser. A **317**, 133 (1970).
[23] H. Yamada-Kaneta, C. Kaneta, and T. Ogawa, Phys. Rev. B **42**, 9650 (1990).
[24] R. Jones, A. Umerski, and S. Öberg, Phys. Rev. B **45**, 11321 (1992).
[25] B. Pajot, E. Artacho, C. A. Ammerlaan, and J.-M. Spaeth, J. Phys.: Condens. Matter **7**, 7077 (1995).
[26] M. Pesola, J. von Boehm, T. Mattila, and R. M. Nieminen, Phys. Rev. B **60**, 11449 (1999).
[27] E. Artacho, F. Ynduráin, B. Pajot, R. Ramírez, C. P. Herrero, L. I. Khirunenko, K. M. Itoh, and E. E. Haller, Phys. Rev. B **56**, 3820 (1997).
[28] J. Coutinho, R. Jones, P. R. Briddon, and S. Öberg, Phys. Rev. B **62**, 10824 (2000).
[29] R. S. Leigh and R. C. Newman, Semicond. Sci. Technol. **3**, 84 (1988).
[30] R. C. Newman, *Infra-red Studies of Crystal Defects* (Taylor & Francis Ltd, London, 1973).
[31] E. B. Wilson, J. C. Decius, and P. C. Cross, *Molecular Vibrations: The Theory of Infrared and Raman Vibrational Spectra* (Dover, New York, 1980).
[32] E. Sozontov, L. X. Cao, A. Kazimirov, V. Kohn, M. Konuma, M. Cardona, and J. Zegenhagen, Phys. Rev. Lett. **86**, 5329 (2001).
[33] A. A. Kaplyanskii, Opt. Spectrosc. **16**, 329 (1964).
[34] M. Budde, B. Bech Nielsen, R. Jones, J. Goss, and S. Öberg, Phys. Rev. B **54**, 5485 (1996).
[35] M. D. McCluskey and E. E. Haller, Phys. Rev. B **56**, 9520 (1997).
[36] P. R. Briddon and R. Jones, Phys. Status Solidi B **207**, 131 (2000).
[37] S. Goedecker, M. Teter, and J. Hutter, Phys. Rev. B **54**, 1703 (1996).
[38] C. Hartwigsen, S. Goedecker, and J. Hutter, Phys. Rev. B **58**, 3641 (1998).
[39] H. J. Monkhorst and J. D. Pack, Phys. Rev. B **13**, 5188 (1976).
[40] R. Jones, in *Identification of Defects in Semiconductors*, edited by M. Stavola, Semiconductors and Semimetals, Vol. 51A (Academic Press, San Diego, 1998), p. 288.
[41] C. G. Van de Walle, Y. Bar-Yam, and S. T. Pantelides, Phys. Rev. Lett. **60**, 2761 (1988).
[42] R. Jones, B. J. Coomer, B. Hourahine, and A. Resende, Solid State Phenom. **71**, 173 (2000).
[43] A. Balsas, V. J. B. Torres, J. Coutinho, R. Jones, B. Hourahine, P. R. Briddon, and M. Barroso, J. Phys.: Condens. Matter **17**, S2155 (2005).